Molecular Pharmacology Fast Forward. Published on August 16, 2010 as doi:10.1124/mol.110.065961

Mol #65961

Amurensin G, a potent natural SIRT1 inhibitor, rescues doxorubicin responsiveness via down-regulation of multidrug resistance 1

Won Keun Oh, Kyoung Bin Cho, Tran Thi Hien, Tae Hyung Kim, Hyung Sik Kim, Trong Tuan Dao, Hyo-Kyung Han, Seong-Min Kwon, Sang-Gun Ahn, Jung-Hoon Yoon, Tae Hyun Kim, Yoon Gyoon Kim, Keon Wook Kang

BK21 Project Team, College of Pharmacy, Chosun University, Gwangju 501-759 (W.K.O., K.B.C., T.T.H., T.T.D., K.W.K.); College of Pharmacy, Pusan National University, Busan 609-735 (T.H.K., H.S.K.); Department of Pathology and Research Center for Oral Disease Regulation of the Aged, College of Dentistry, Chosun University, Gwangju 501-759 (S.K., S.A., J.Y.); Department of Pharmacology, College of Medicine, Dankook Univeristy, Cheonan 330-714 (T.H.K., Y.G.K.), Republic of Korea.

Molecular Pharmacology Fast Forward. Published on August 16, 2010 as DOI: 10.1124/mol.110.065961
This article has not been copyedited and formatted. The final version may differ from this version.

Running title: Down-regulation of MDR1 by amurensin G, a SIRT1 inhibitor

Corresponding author: Keon Wook Kang, Ph.D. College of Pharmacy, Chosun University, 375 Seosuk-dong, Dong-gu, Gwangju 501-759, South Korea; E-mail: kwkang@chosun.ac.kr

Document Statistics

Number of text pages: 39

Number of tables: 0

Number of figures: 5

Number of references: 38

Number of words in the abstract: 240

Number of words in the introduction: 593

Number of words in the discussion: 957

Abbreviations: ABC, ATP-binding cassette; BCRP, breast cancer resistance protein; DMEM, Dulbecco's modified Eagle's medium; FBS, fetal bovine serum; DTT, dithiothreitol; FHRE, Forkhead-response element; FoxO, Forkhead box-containing protein of the O subfamily; HEPES, 4-(2-hydroxyethyl)-1-piperazineethanesulfonic acid; MCF-7/ADR, adriamycin-resistant breast cancer cells; MDR, multi-drug resistance; MRP, multidrug resistance-associated protein; MTT, 3-(4,5-dimethylthiazol-2-yl)- 2,5-diphenyl-tetrazolium bromide; PBS, phosphate buffered saline; PCNA, proliferating cell nuclear antigen; PI3-kinase, phosphatidylinositol 3-kinase; PMSF, phenylmethylsulfonylfluoride; PXR, pregnane X receptor; R-123, Rhodamine-123; SIRT1, silent information regulator two ortholog 1; TUNEL, TdT mediated dUTP nick end labeling

Molecular Pharmacology Fast Forward. Published on August 16, 2010 as DOI: 10.1124/mol.110.065961
This article has not been copyedited and formatted. The final version may differ from this version.

ABSTRACT

The transition from a chemotherapy-responsive cancer to a chemotherapy-resistant one is accompanied by increased expression of multi-drug resistance 1 (MDR1, p-glycoprotein), which plays an important role in the efflux from the target cell of many anti-cancer agents. We recently showed that a Forkhead box-containing protein of the O subfamily 1 (FoxO1) is a key regulator of MDR1 gene transcription. Because nuclear localization of FoxO1 is regulated by silent information regulator two ortholog 1 (SIRT1) deacetylase, we wondered whether SIRT1 dominates MDR1 gene expression in breast cancer cells. Overexpression of SIRT1 enhanced both FoxO reporter activity and nuclear levels of FoxO1. Protein expression of MDR1 and gene transcriptional activity were also up-regulated by SIRT1 overexpression. In addition, SIRT1 inhibition reduced both nuclear FoxO1 levels and MDR1 expression in adriamycin-resistant breast cancer cells (MCF-7/ADR) cells. A potent SIRT1 inhibitor, amurensin G (from *Vitis amurensis*), was identified by screening plant extracts and bioassay-guided fractionation. The compound suppressed FoxO1 activity and MDR1 expression in MCF-7/ADR cells. Moreover, pretreatment of MCF-7/ADR cells with 1 μg/ml amurensin G for 24 h increased cellular uptake of doxorubicin and restored the responsiveness of MCF-7/ADR cells to doxorubicin. In xenograft studies, intraperitoneal injection of 10 mg/kg amurensin G substantially restored the ability of doxorubicin to inhibit MCF-7/ADR induced tumor growth. These results suggest that SIRT1 is a potential therapeutic target of MDR1-mediated chemoresistance and it may be possible to develop amurensin G as a useful agent for chemoresistance reversal.

Molecular Pharmacology Fast Forward. Published on August 16, 2010 as DOI: 10.1124/mol.110.065961
This article has not been copyedited and formatted. The final version may differ from this version.

INTRODUCTION

Although chemotherapy is widely used for the treatment of various cancers, its use is frequently limited by acquisition by tumor cells of multidrug resistance (MDR). MDR describes a phenomenon of resistance not only to the current drug but also to structurally different chemotherapeutic agents (Ozben, 2007). One of the most important mechanisms underlying resistance to chemotherapy is the active efflux of anti-cancer drugs through increased expression of the ATP-binding cassette (ABC) transporters (Bodó et al., 2003; Pérez-Tomás, 2006). There are three well-known MDR genes that have been identified in humans: (a) multi-drug resistance 1 (MDR1, p-glycoprotein, ABCB1), (b) multidrug resistance-associated proteins (MRPs, ABCC subfamily) and (c) breast cancer resistance protein (BCRP, ABCG2) (Kuo, 2007). ABC transporters are transmembrane proteins that pump out a number of molecules across cellular membranes using ATP binding. Though there may be some differences among them, these transporters commonly have been known to cause the efflux of a variety of anti-tumor agents (Glavinas et al., 2004). However, the expression mechanisms of ABC transporters have not been fully understood despite obvious expression of these proteins in most tumor tissues. Moreover, attempts to modulate the activity of these proteins have met with limited success (Ozben, 2007).

Forkhead box-containing protein, O subfamily (FoxO) transcription factors hold a conserved DNA binding domain termed the Forkhead box. Four proteins – FoxO1, FoxO3, FoxO4 and FoxO6 – have been identified as members of the O subfamily FoxO in mammals, and transcriptional activity of FoxO factors is regulated by a shuttling system running between the nucleus and the cytoplasm. This system can be regulated by phosphorylation-dependent ubiquitination and acetylation (Barthel et al., 2005; Vogt et al., 2005; Hoekman et al., 2006). A variety of cellular fates such as differentiation, metabolism and proliferation are controlled by FoxO factors (Accili and Arden, 2004), and these are frequently dysregulated in some cancers (Barthel et al., 2005; Arden, 2006). We recently found that FoxO1 is consistently up-regulated in MCF-7/ADR, adriamycin-resistant breast cancer cells, and FoxO1 plays a critical role in the expression of the MDR1 gene (Han et al., 2008).

Silent information regulator two ortholog 1 (SIRT1) is the human ortholog of the yeast sir2 protein, which is the name of a family of closely related enzymes, the sirtuins (Motta et al., 2004; Borra et al., 2005). Sirtuins play a key role in cellular responses to stressors such as heat or starvation, and are responsible for the lifespan-extending processes of calorie restriction (Borra et al., 2005; de Boer et al., 2006). Sirtuins act by removing acetyl groups from proteins in the presence of NAD^+. They are thus classified

Molecular Pharmacology Fast Forward. Published on August 16, 2010 as DOI: 10.1124/mol.110.065961
This article has not been copyedited and formatted. The final version may differ from this version.

as NAD^+-dependent deacetylases (de Boer et al., 2006). Several transcription factors (e.g., p53 and nuclear factor-κB) have been reported to be substrates of SIRT1 (Yeung et al., 2003). FoxO transcription factors are also deacetylated by SIRT1 and consequently are accumulated in the nucleus (Stünkel et al., 2007).

Based on the hypothesis that SIRT1-dependent FoxO1 activity is important for the expression and regulation of ABC transporters, we investigated a potential role for SIRT1 activation in the up-regulation of MDR1 in MCF-7/ADR cells. We also screened for *in vitro* SIRT1 activity using 1,820 plant extracts and found methanol extracts of *Vitis amurensis* has relatively potent SIRT1 inhibitory activity. Bioassay-guided fractionation of this extract resulted in the isolation of eight oligostilbenes and amurensin G showed the most potent SIRT1 inhibition. We then assessed the inhibitory effect of amurensin G on FoxO1-mediated MDR1 expression in MCF-7/ADR cells. We also tested whether amurensin G reversed doxorubicin resistance in a xenograft model generated by transplantation into mice of MCF-7/ADR cells.

MATERIALS AND METHODS

Materials. Anti-MDR1 antibody was supplied by Calbiochem (Darmastadt, Germany). FoxO1 and FoxO3a specific antibodies, SIRT1 antibody, and horseradish

Molecular Pharmacology Fast Forward. Published on August 16, 2010 as DOI: 10.1124/mol.110.065961
This article has not been copyedited and formatted. The final version may differ from this version.

peroxidase-conjugated anti-rabbit and anti-mouse IgGs were purchased from Cell Signaling Technology (Beverly, MA). Alkaline phosphatase-conjugated donkey anti-mouse IgG and horseradish peroxidase-conjugated rabbit anti-goat IgG were provided by Jackson Immunoresearch Laboratories (West Grove, PA). Most of the reagents used for molecular studies were obtained from Sigma (St. Louis, MO). The siRNA targeting human FoxO1 was acquired from Ambion (Austin, TX). Human recombinant SIRT1, Fluor de Lys SIRT1 deacetyalse substrate, Fluor de Lys Developer II NAD+ and the buffer used for assays were purchased from Biomol (Plymouth Meeting, PA). 1,820 of the plant extracts were purchased from 21C Frontier R&D Program Plant Diversity Research Center in Republic of Korea (Supplemental Table 1).

Cell culture. MCF-7 cells and adriamycin-resistant MCF-7 (MCF-7/ADR) cells were cultured in Dulbecco's modified Eagle's medium (DMEM) containing 10% fetal bovine serum (FBS), 100 units/ml penicillin, and 100 μg/ml streptomycin at 37°C in a humidified 5% CO_2 atmosphere.

Plasmids. The p195-MDR1-Luc reporter plasmid was generated by ligating PCR-amplified MDR1 promoter regions with pGL3-enhancer vector (Promega, Madison, WI) (Han et al., 2008). The FHRE-Luc, FoxO response element-containing a reporter plasmid, was acquired from Addgene Inco. (Cambridge, MA). The SIRT1

Molecular Pharmacology Fast Forward. Published on August 16, 2010 as DOI: 10.1124/mol.110.065961
This article has not been copyedited and formatted. The final version may differ from this version.

constitutive active plasmid was kindly donated by Dr. KY Lee (Chonnam National University, Gwangju, Korea).

Preparation of nuclear extracts. Nuclear extracts were prepared essentially as described by Schreiber et al (Schreiber et al., 1990). Briefly, cells in dishes were washed with ice-cold PBS, scraped, transferred to microtubes, and allowed to swell after adding 100 μl of lysis buffer containing 10 mM 4-(2-hydroxyethyl)-1-piperazineethanesulfonic acid (HEPES, pH 7.9), 0.5% Nonidet P-40, 10 mM KCl, 0.1 mM EDTA, 1 mM dithiothreitol (DTT) and 0.5 mM phenylmethylsulfonylfluoride (PMSF). Cell membranes were disrupted by vortexing, and the lysates were incubated for 10 min on ice and centrifuged at 7,200 g for 5 min. Pellets containing crude nuclei were resuspended in 60 μl of extraction buffer containing 20 mM HEPES (pH 7.9), 400 mM NaCl, 1 mM EDTA, 1 mM DTT and 1 mM PMSF, and then incubated for 30 min on ice. The samples were then centrifuged at 15,800 g for 10 min to obtain supernatants containing nuclear extracts, which were stored at -80°C until required.

Immunoblot analysis. After washing with sterile phosphate buffered saline (PBS), MCF-7 and MCF-7/ADR cells were lysed in EBC lysis buffer containing 20 mM Tris·Cl (pH 7.5), 1% Triton X-100, 137 mM sodium chloride, 10% glycerol, 2 mM EDTA, 1 mM sodium orthovanadate, 25 mM -glycerophosphate, 2 mM sodium

Molecular Pharmacology Fast Forward. Published on August 16, 2010 as DOI: 10.1124/mol.110.065961
This article has not been copyedited and formatted. The final version may differ from this version.

pyrophosphate, 1 mM PMSF, and 1 μg/ml leupeptin. Cell lysates were centrifuged at 10,000 *g* for 10 min to remove debris, and proteins were fractionated using a 10% separating gel. The fractionated proteins were then transferred electrophoretically to nitrocellulose paper and immunoblotted with specific antibodies. Horseradish peroxidase- or alkaline phosphatase-conjugated anti-IgG antibodies were used as the secondary antibodies. The nitrocellulose papers were developed using 5-bromo-4-chloro-3-indolylphosphate (BCIP)/4-nitroblue tetrazolium (NBT) or an ECL chemiluminescence system. For chemiluminescence detection, the LAS3000-mini (Fujifilm, Tokyo, Japan) was used.

Reporter gene assay. Promoter activity was determined using a dual-luciferase reporter assay system (Promega, Madison, WI). Briefly, cells (3×10^5 cells/well) were replated in 12-well plates overnight and transiently transfected with FHRE-Luc or p195-MDR1 reporter plasmid/phRL-SV plasmid (hRenilla luciferase expression for normalization) (Promega, Madison, WI) using Hilymax® reagent (Dojindo Molecular Technologies, Gaithersburg, MD). Cells were then incubated in the culture medium without serum for 18 h, and the firefly and hRenilla luciferase activities in the cell lysates were measured using a luminometer (LB941, Berthold Technologies, Bad Wildbad, Germany). The relative luciferase activities were calculated by normalizing

the promoter-driven firefly luciferase activity versus hRenilla luciferase.

Amurensin G isolation. The stem of *V. amurensis* was collected in July 2008 in Mai moutain, Jinan-Gun, Jeollabuk-do, Republic of Korea. The sample was authenticated by Professor YH Moon at Chosun University, and a voucher specimen (No. CU-0235) was deposited at the herbarium of Chosun University, Gwangju, Korea. The dried stem (2 kg) of *V. amurensis* was extracted with methanol (10 L × 72 h × 2) at room temperature and the solution was concentrated to obtain a crude extract (250 g). The extract was suspended in H_2O, partitioned successively with *n*-hexane (1.5 L × 3), EtOAc (1.5 L × 3), and BuOH (1.5 L × 3). The EtOAc fraction (87 g) was subjected to silica gel column chromatography (10 × 35 cm; 63–200 μm particle size) using *n*-hexane/acetone gradient (from 5:1 to 0:1) to give seven fractions (F1–F7) based on the TLC profile. Fraction 6 (20.5 g) was divided into 3 fractions (F6.1–F6.3) by a column of Sephadex LH-20 using MeOH as the mobile phase. Fraction F6.2 (5.5 g) was then applied to C-18 silica gel column chromatography and eluted with a step gradient of MeOH/H_2O (from 1:1 to 10:1) to afford six subfractions (F6.2.1–F6.2.6). Subfraction F6.2.3 (300 mg) was subjected to HPLC with an ODS-H80 column [(20 × 150 mm, 4 μm particle size); solvent MeOH in H_2O containing 0.1 % formic acid (0 – 25 min: 35 % MeOH, 35 min: 100 % MeOH); flow rate 3 mL/min; UV detection at 280 and 320

Molecular Pharmacology Fast Forward. Published on August 16, 2010 as DOI: 10.1124/mol.110.065961
This article has not been copyedited and formatted. The final version may differ from this version.

nm] to give amurensin G (t_R = 20 min, 28 mg). **Amurensin G;** Brown amorphous powder; mp 263-264 °C; $[\alpha]_D^{25}$ +28° (*c* 0.1, MeOH); UV (MeOH) λ_{max} (log ε) 213 (3.80), 217 (3.95), 224 (4.00), 282 (4.32) nm; IR (film) ν_{max} 3320, 1610, 1510, 1180, 1040, 840 cm^{-1}; ^1H- and ^{13}C-NMR were in accordance with reported data; EI-MS *m/z* 681 $[M + H]^+$ (Calc. for $C_{42}H_{32}O_9$).

SIRT1 deacetylase enzyme assay. The Fluor de Lys fluorescence assay was used to assess SIRT1 activity of phytochemicals. The Fluor de Lys fluorescence assay was performed as described in the BioMol product sheets (Borra et al., 2005). Briefly, assays were performed using Fluor de Lys-SIRT1, NAD+, SIRT1 enzyme in SIRT1 assay buffer (50 mM Tris-Cl, pH 8.0, 137 mM NaCl, 2.7 mM KCl, 1 mM $MgCl_2$, 1 mg/ml bovine serum albumin). After preincubating the assay buffer with the SIRT1 enzyme for 10 min, the reaction was initiated by the addition of the Fluor de Lys peptide and NAD^+. After 45 min incubation, 2 mM nicotinamide was added to Developer II in the histone deacetylase assay buffer (25 mM Tris/Cl pH 8.0, 137 mM NaCl, 2.7 mM KCl, and 1 mM $MgCl_2$). At each time point, 50 µL of the reaction was removed and mixed with 50 µL of the developer solution. Finally, the fluorescence was measured using a microplate reader (Varioskan, Thermo Electron Co.) with the excitation and emission at λ=360 nm and λ=460 nm, respectively.

MTT cell viability assay. To determine cell viability, cells were plated at 10^4 cells/well in 96-well plates. For determination of the cytotoxicity of amurensin G, MCF-7/ADR cells were incubated in FBS-free medium with or without amurensin G (0.1–3 μg/ml) for 24 h. Viable adherent cells were stained with 3-(4,5-dimethylthiazol-2-yl)- 2,5-diphenyl-tetrazolium bromide (MTT; 2 mg/ml) for 4 h. The media were then removed and the formazan crystals produced were dissolved by adding 200 μl dimethylsulfoxide/well. Absorbance was assayed at 540 nm. Cell viability was expressed as relative ratios to untreated control cells.

Crystal violet assay. Doxorubicin-induced cell death was determined by crystal violet staining (Vellonen et al., 2004). Cells were stained with 0.4% crystal violet in methanol for 30 min at room temperature and then washed with tap water. Stained cells were extracted with 50% methanol and dye extracts were measured at 550 nm using a microtiter plate reader (Berthold Technologies, Bad Wildbad, Germany).

Cellular uptake of doxorubicin. Doxorubicin uptake was quantified in MCF-7 and MCF-7/ADR cells. Cells ($3x10^6$ cells) were incubated with 30 μM doxorubicin for 60 min, washed with PBS three times, and lysed in EBC lysis buffer containing 20 mM Tris·Cl (pH 7.5), 1% Triton X-100, 137 mM sodium chloride, 10% glycerol, 2 mM EDTA, 1 mM sodium orthovanadate, 25 mM β-glycerophosphate, 2 mM sodium

Molecular Pharmacology Fast Forward. Published on August 16, 2010 as DOI: 10.1124/mol.110.065961
This article has not been copyedited and formatted. The final version may differ from this version.

pyrophosphate, 1 mM PMSF, and 1 μg/ml leupeptin. After centrifugation of the samples at 10,000 *g* for 10 min, change in fluorescent absorbance of doxorubicin in the supernatant was determined at excitation and emission wavelengths of 470 nm and 590 nm, respectively. Uptake intensity was expressed as a relative ratio to the fluorescence value for the doxorubicin-treated group.

Determination of cellular concentration of doxorubicin. For the determination of cellular concentration of doxorubicin, cell lysates were collected as described in 'cellular uptake of doxorubicin' part. 200-μl of acetonitrile with internal standard (ε-acetoaminocarproic acid, 1 μg/ml) was added to the 50 μl of cell lysate and the mixture was vortexed for 15 sec and then centrifuged for 5 min at 12,000 rpm. The organic layer was transferred to another tube and dried under nitrogen flow. The dried sample was then reconstituted with 120 μl of solvent (0.1% formic acid in 30% acetonitrile solution), vortexed and 50 μl was transferred to autosample vial and 5 μl injected into the HPLC system. An aliquot (5 μl) of each sample extract was injected into a Gemini-NX C_{18} analytical column (150×2.0 mm i.d.). The compounds were eluted by pumping the mobile phase (10 mM ammonium formate in water:acetonitrile=70:30, v/v) at a flow rate of 300 μl/min. Under this conditions, typical standard retention time was 1.2 min and 1.5 min for internal standard and doxorubicin, respectively. Total chromatographic

run time was 3.5 min. The mass spectrometer (LC/MS/MS 1200L, Varian, CA) equipped with an electrospray source in positive mode was set up in multiple reaction monitoring (MRM), monitoring the transitions 544.2>361.0 with collision energy 25 eV for doxorubicin and 174.0>114.1 with collision energy 14 eV for internal standard.

TdT mediated dUTP nick end labeling (TUNEL) assay. TUNEL assays were performed using an *in situ* cell death detection kit (Roche Diagnostics GmbH, Germany). After 18 h of incubation with either doxorubicin (30 μM) or amurensin G (0.3-1 μg/ml), MCF-7 or MCF-7/ADR cells were washed with PBS. Cells on slides were then fixed with 4% paraformaldehyde in PBS (pH 7.4) for 1 h at room temperature, and then permeabilized with 0.1% Triton® X-100 in 0.1% sodium citrate for 2 min on ice. They were then washed with PBS, incubated for 60 min at 37°C after adding 50 μl of TdT enzyme solution, incubated for 30 min at 37°C after adding 50 μl of anti-fluorescent antibody (Fab fragment from sheep conjugated with alkaline phosphatase), and further incubated for 10 min in the presence of BCIP/NBT solution. Slides were then rinsed with phosphate-buffered saline, mounted under cover-slips, and analyzed under an optical microscope.

Xenograft study. A mouse xenograft model was established using **s**ix week-old female BALB/c nude mice (Central Lab. Animal Inc., Seoul, Korea). Tumor cells

Molecular Pharmacology Fast Forward. Published on August 16, 2010 as DOI: 10.1124/mol.110.065961
This article has not been copyedited and formatted. The final version may differ from this version.

(5×10^6 MCF-7/ADR cells) were suspended in 0.1ml serum-free medium containing 50% Matrigel and injected subscutaneously into the upper flank of each nude mice. When tumors reached approximately 200 mm^3 (at about 12 days), mice were randomly allocated to the vehicle control, doxorubicin-treated or the amurensin G + doxorubicin-treated groups. Two weeks after inoculation, 0.1 ml of amurensin G solution (10mg/kg) were intraperitoneally injected for four weeks [twice a week (Monday & Tuesday)] and doxorubicin was also intraperitoneally given at 4 mg/kg for four weeks [one time a week (Wednesday)]. Tumor volumes were measured as described previously (Ahn et al., 2010). The animal protocol used in this study has been reviewed by the Pusan National University–Institutional Animal Care and Use Committee (PNU-IACUC) on their ethical procedures and scientific care, and it has been approved (Approval Number PNU-2009-0024).

After sacrificing the mice, excised tumors were fixed in 10% buffered formalin and embedded in paraffin. For the pathology examination, 4 μm thick tissue sections were stained with H&E. Immunohistochemical staining was done with the avidin-biotin complex method using an anti-proliferating cell nuclear antigen (PCNA) antibody. Immune reactions were visualized with 3,3-diaminobenzidine and counterstained with Mayer's hematoxylin. Tissue TUNEL assays were performed using ApopTag Plus

Peroxidase In Situ Apoptosis Detection kits (Intergen, Purchase, NY) according to the manufacturer's instructions. Briefly, slides were deparaffinized and immersed in 3% hydrogen peroxide to block endogenous peroxidase. Then, slides were incubated with reaction buffer containing terminal deoxynucleotidyl transferase at 37°C for 1 h. Slides were then incubated with peroxidase-conjugated anti-digoxigenin antibody for 30 min, and the reaction products were visualized with 0.03% 3,3-diaminobenzidine solution containing 2 mmol hydrogen peroxide. Counterstaining was achieved with 0.5% methyl green. The PCNA and TUNEL-positive cells were counted and represented as the average of the five highest areas within a single x200 field. A portion of tumor tissues was homogenized and subjected to immunoblotting for MDR1.

Statistical analysis. Scanning densitometry was performed using an LAS-3000mini (Fujifilm, Japan). One way analysis of variance (ANOVA) procedures were used to assess the significance of differences between treatment groups. When treatment was found to have a significant effect, the Newman-Keuls test was used to compare multiple group means. Statistical significance was accepted at either $p<0.05$ or $p<0.01$.

RESULTS

Molecular Pharmacology Fast Forward. Published on August 16, 2010 as DOI: 10.1124/mol.110.065961
This article has not been copyedited and formatted. The final version may differ from this version.

Involvement of SIRT1 in FoxO1-dependent MDR1 expression. In our previous study, we showed that FoxO1 binding to the MDR1 promoter plays a key role in MDR1 expression in MCF-7/ADR cells (Han et al., 2008). FoxO factors can be controlled by two different mechanisms: phosphorylation and acetylation. Multiple kinase pathways including phosphatidylinositol 3-kinase (PI3-kinase)/Akt, extracellular signal regulated kinase and p38 kinase have been shown to regulate FoxO via phosphorylation (Vogt et al., 2005; Asada et al., 2007). It has also been reported that SIRT1 causes nuclear translocation of FoxO1 via its deacetylation, and subsequently increases the transcriptional activity of FoxO1 (Frescas et al., 2005). Because SIRT1 is considered to be a promising target for anti-cancer agent development (Saunders et al., 2007), we were interested in the potential involvement of SIRT1 in MDR1 gene transcription.

We first examined whether SIRT1 activity is essential for FoxO1-dependent MDR1 expression. Both the reporter activity of p195-MDR1-Luc containing a FoxO1 binding site (Han et al., 2008) and the MDR1 protein levels were significantly elevated by overexpression of SIRT1 constitutive active plasmids in MCF-7 cells (Fig. 1A). Also, SIRT1 overexpression selectively increased nuclear levels of FoxO1 and the transcriptional activity of the forkhead-response element (FHRE) minimal reporter (Fig.

1B). Moreover, 1 mM nicotinamide, a representative SIRT inhibitor, inhibited nuclear accumulation of FoxO1 and reduced levels of MDR1 protein in MCF-7/ADR cells (Fig. 1C, left). These results clearly demonstrate that SIRT1 activity is closely connected with the expression of FoxO1-mediated MDR1. We further examined the transport activity of MDR1 using a Rhodamine-123 (R-123, a substrate of MDR1) retention assay. The reduced accumulation of R-123 in MCF-7/ADR cells was significantly reversed by 1 mM nicotinamide (Fig. 1C, right). This indicates that MDR1 activity as well as its expression is controlled by SIRT1 deacetylase.

Synergistic effects of SIRT1 on FoxO1-dependent MDR1 expression. To confirm whether SIRT1 regulates FoxO1-mediated MDR1 gene transcription, MCF-7 cells were co-transfected with constitutively active SIRT1 plasmids with or without a FoxO1 overexpression plasmid. SIRT1 overexpression in the presence of FoxO1 synergistically enhanced both the promoter activity and the protein expression of MDR1 as did FoxO1 overexpression alone (Fig. 2A). Furthermore, SIRT1-induced MDR1 protein expression or MDR1 transcription was reversed by FoxO1 siRNA (Fig. 2B). These data support the idea that SIRT1 is a critical regulator of MDR1 expression via a FoxO1-dependent mechanism and FoxO1 and SIRT1 cooperate with each other to

induce MDR1 expression.

Screening for potent SIRT1 inhibitors from natural sources and the MDR1 inhibiting effect of amurensin G. Because SIRT1 controls the cell cycle and apoptosis during tumorigenesis (Saunders et al., 2007), and considering SIRT1's critical role in the regulation of MDR1 expression, the deacetylase could be an attractive anti-cancer targets. Although several SIRT inhibiting chemicals have been identified, potential toxicity or low efficacy is a main obstacle to developing new anti-cancer agents. Hence, we tried to identify potent SIRT1 inhibitors from 1,820 plant extracts and found that methanol extracts of *Vitis amurensis* has significant SIRT1 inhibitory activity (35% inhibition at 30 μg/mL). Active compound with SIRT1 inhibitory activity was isolated by bioassay-guided fractionation from *Vitis amurensis* methanol extracts. Active compound was obtained as a brown amorphous powder. Its EI-MS gave the $[M + H]^+$ ion at *m/z* 681, and the molecular formula of $C_{42}H_{32}O_9$ was inferred from an analysis of the ^1H and ^{13}C NMR spectra. The ^1H NMR spectrum of active compound showed three sets of signals for 4-hydroxybenzene moieties, one set of signals for a 3,5-dihydroxybenzene moiety, two *meta*-coupled doublets due to two aromatic protons, a singlet for an aromatic proton, and six aliphatic protons. Based on an analysis of the

Molecular Pharmacology Fast Forward. Published on August 16, 2010 as DOI: 10.1124/mol.110.065961
This article has not been copyedited and formatted. The final version may differ from this version.

spectra and reported data (Ha et al., 2009), active compound was identified as amurensin G, which is a resveratrol trimer (Fig. 3A).

Amurensin G showed *in vitro* inhibitory effects superior to that of 1 mM nicotinamide on SIRT1 enzyme activity (Fig. 3B, left). We then tested the inhibitory effect of amurensin G on SIRT1/FoxO1-dependent transcriptional activity using a FHRE reporter plasmid. After enhancing FHRE reporter activity by introducing a constitutively active SIRT1 plasmid, MCF-7 cells were exposed to amurensin G. Amurensin G reduced SIRT1-induced FHRE transcriptional activity in a concentration dependent manner and 1 μg/ml amurensin G was enough to completely suppress SIRT1-dependent FHRE reporter activity (Fig. 3B, right). To determine whether amurensin G suppresses MDR1 expression, western blot analysis was performed. The compound potently inhibited the expression of MDR1 in MCF-7/ADR cells (Fig. 3C). Moreover, nuclear FoxO1 levels were attenuated by amurensin G treatment, while FoxO3 was not altered (Fig. 3C). We then determined the basal cytotoxicity of amurensin G in MCF-7/ADR cells. MTT assay revealed that amurensin G up to 3 μg/ml did not alter the viability of cells (Fig. 3D).

Enhanced doxorubicin uptake and synergistic cytotoxicity by amurensin G.

Molecular Pharmacology Fast Forward. Published on August 16, 2010 as DOI: 10.1124/mol.110.065961
This article has not been copyedited and formatted. The final version may differ from this version.

Next, we tested whether the cellular uptake of doxorubicin was enhanced by amurensin G using fluorescence detection (Fig. 4A) or LC/Ms/Ms-based cellular concentration determination (Fig. 4B). Doxorubicin was accumulated in MCF-7/ADR cells to a lesser extent than in MCF-7 cells. Whereas, doxorubicin uptake in MCF-7/ADR cells was enhanced with increasing concentrations of amurensin G (Fig. 4A and 4B). We further determined whether doxorubicin responsiveness is rescued by amurensin G1 in cell culture study. After a 24 h preincubation of MCF-7/ADR cells with vehicle or amurensin G (0.1, 0.3, 1 μg/ml), doxorubicin (30 μM)-mediated cell death was monitored. Amurensin G treatment significantly enhanced the cytotoxicity of doxorubicin, as evidenced by crystal violet (Fig. 4C) and BrdU uptake (Fig. 4D) assays. Moreover, TUNEL staining showed that exposure of control MCF-7 cells to doxorubicin (30 μM) for 24 h caused severe apoptosis, but not in MCF-7/ADR cells (Fig. 4E). However, TUNEL-positive cells were again found in MCF-7/ADR cells pretreated with amurensin G (0.3 or 1 μg/ml) for 24 h (Fig. 4E) suggesting the MDR1 down-regulatory effect of amurensin G restores cell sensitivity to doxorubicin. We next determined the possible synergistic effect of amurensin G on paclitaxel-mediated cell proliferation inhibition in MCF-7/ADR cells. As expected, amurensin potentiated paclitaxel-mediated cytotoxicity in a concentration-dependent manner (Fig. 4F).

Molecular Pharmacology Fast Forward. Published on August 16, 2010 as DOI: 10.1124/mol.110.065961
This article has not been copyedited and formatted. The final version may differ from this version.

Restoration of doxorubicin responsiveness by amurensin G in xenograft studies.

We assessed tumor growth in athymic nude mice bearing MCF-7/ADR cells. Four mg/kg doxorubicin treatment (once per week for 4 weeks) only showed marginal inhibition of tumor growth, but co-injection of amurensin G (10 mg/kg, two times a week) significantly potentiated doxorubicin-mediated inhibition of tumor growth (Fig. 5A). On histological examination, the tumor showed solid growth of undifferentiated carcinoma devoid of glandular or ductal differentiation. However, amurensin G co-treated tumor led to extensive cell death than control or doxorubicin alone treated tumor (Fig. 5B). PCNA is a representative marker for cancer cell proliferation. Immunohistochemical analysis showed that all of the tumor cells in the vehicle-treated control cells and in cells treated with doxorubicin alone were PCNA-positive, while the number of PCNA-positive cells was significantly decreased when cells were co-treated with amurensin G (Fig. 5B). PCNA is not expressed in throughout the whole cell cycle, Ki-67 tumor-specific antigen is expressed in proliferative cells throughout the G1, S, G2 and M phase. Hence, immunohistochemical Ki-67 staining can provide a reliable index of tumor cell proliferation (Brown et al., 1990). Ki-67 staining intensity was also decreased by amurensin G cotreatment with doxorubicin (Fig. 5B). Moreover, co-

Molecular Pharmacology Fast Forward. Published on August 16, 2010 as DOI: 10.1124/mol.110.065961
This article has not been copyedited and formatted. The final version may differ from this version.

treatment with amurensin G enhanced the number of TUNEL-positive cells (Fig. 5B). We then measured MDR1 protein expression in tumor tissue lysates. MDR1 protein expression was clearly decreased in amurensin G-treated samples (Fig. 5C). These results confirm our cell culture data that the natural SIRT1 inhibitor, amurensin G, strongly inhibits the growth of MCF-7/ADR-derived tumors by MDR1 down-regulation.

DISCUSSION

Multi-drug resistance is a serious obstacle in the treatment of breast cancer (Liu et al., 2007). Several ABC-superfamily multidrug efflux pumps are known to be involved in this phenomena. MDR1 and MRPs are the overt proteins to drive this severe resistance (Ling, 1997; Sharom, 2008). Although these efflux systems can help in removing harmful chemicals and protecting tissues from toxic materials, a more serious problem is the management of patients who are taking chemotherapeutic drugs, patients whose fate is at the crossroads of life and death. What is worse, these proteins have intersecting effects on other unrelated anti-cancer agents, resulting in low success of treatment (Lage, 2003). Hence, extensive studies have been performed to identify chemical MDR1 inhibitors to improve uptake of anticancer drugs. In fact, many MDR1

Molecular Pharmacology Fast Forward. Published on August 16, 2010 as DOI: 10.1124/mol.110.065961
This article has not been copyedited and formatted. The final version may differ from this version.

activity inhibitors have been developed by pharmaceutical companies. However, MDR1 activity inhibitors frequently cause severe side effects or interfere with the kinetics of other drugs (Zhou et al., 2006). Hence, two different approaches have been suggested to overcome MDR1-mediated drug efflux; humanized monoclonal antibody therapy targeting MDR1 or development of novel inhibitors to target MDR1 gene expression (Gottesman et al., 2002). In this paper, we demonstrate that SIRT1 inhibitor may functions as one of efficient adjuvant chemotherapies to suppress MDR1 expression as well as cell proliferation.

FoxO plays an important role in cell growth, proliferation, differentiation, longevity, metabolism and tumor development (Accili and Arden, 2004; Barthel et al., 2005; Arden, 2006; Reagan-Shaw et al., 2007). In our previous study, we showed that FoxO1 binding to the -150 ~ -144 bp MDR1 gene promoter is a key event in the transactivation of the MDR1 gene in MCF-7/ADR cells which suggested that FoxO1 could be a target for multidrug resistance (Han et al., 2008). The activity of FoxO is controlled by post-translational modifications, including phosphorylation/ubiquitination and acetylation (Vogt et al., 2005). Activation of a representative cell proliferation signal, PI3-kinase/Akt phosphorylates FoxO1 and subsequently causes ubiquitination-dependent degradation (Vogt et al., 2005). Thus, activation of PI3-kinase may reduce

Molecular Pharmacology Fast Forward. Published on August 16, 2010 as DOI: 10.1124/mol.110.065961
This article has not been copyedited and formatted. The final version may differ from this version.

FoxO1 activity, but it also could result in cancer cell proliferation.

SIRT1, a member of the sirtuin family, is known to be a regulator of lifespan extension. SIRT1 acts as one of the critical regulators of FoxO transcription in response to cellular stress via its role in NAD-dependent deacetylation (Gan et al., 2005). Frescas et al. suggested that deacetylation of FoxO by SIRT1 increases its nuclear retention time and thus increases transcriptional activity (Frescas et al., 2005). On the other hand, Motta et al. insisted that SIRT1 down-regulates and represses forkhead factor, including FoxO1 and FoxO4, as well as FoxO3a by destabilizing the protein, decreasing its DNA binding activity, or changing protein/protein interactions (Motta et al., 2004).

Although there is a controversy about SIRT1-mediated FoxO regulation mechanism, recent studies showed SIRT1 to be an enhancer of FoxO activation. SIRT1-mediated deacetylation blocks FoxO inhibition introduced from acetylation, and thereby prolongs FoxO-dependent transcription of subnuclear stress-regulating genes. Through this mechanism, SIRT1 is thought to be able to promote cellular survival and increase lifespan (Daitoku et al., 2004; Kobayashi et al., 2005). In our study, we found that SIRT1 overexpression increases MDR1 gene transcription through nuclear accumulation of FoxO1 in MCF-7 cells. When SIRT1 was co-transfected with FoxO1, MDR1 transcriptional activities were significantly potentiated. Furthermore, MDR1

elevation caused by SIRT1 was reversed by FoxO1 suppression. Vice versa, SIRT1 inhibitors reduced protein levels and promoter activity of FoxO1 and MDR1 in MCF-7/ADR cells. These results clearly demonstrate that SIRT1 is an upstream regulator of FoxO1 and plays a critical role in the up-regulation of the MDR1 gene.

A series of recent studies have suggested that SIRT1 is involved in tumorigenesis, and SIRT1 inhibitors evoked cancer-specific apoptosis (Ota et al., 2006; Alcaín et al., 2009; Lara et al., 2009). However, since only a few SIRT1 inhibitors from natural sources have been reported (Grozinger et al., 2001), identifying a potent SIRT1 inhibitor is meaningful for the development of curative agents against chemotherapy-resistant cancer. In an effort to discover regulators of human SIRT1 enzymes, we screened a phytochemical library using an *in vitro* SIRT1 enzyme assay system. Of 1,820 plant extracts, amurensin G isolated from *Vitis amurensis* methanol extracts showed the most potent inhibition of SIRT1. Interestingly, structure of amurensin G is a trimer of resveratrol known as SIRT1 enzyme activator. The high expression levels of MDR1 and nuclear FoxO1 in MCF-7/ADR cells were drastically reduced by amurensin G treatment. The MDR1 decreasing effects turned out to be due to FoxO1 inhibition as shown by the abilities of amurensin G to reduce FHRE reporter activity and nuclear FoxO1 accumulation. Moreover, our data showing increased doxorubicin cellular

uptake and restoration of doxorubicin-induced apoptosis after treating with amurensin G suggest that the compound is an efficient agent for inhibiting MDR1. MCF-7/ADR cell-implanted xenograft studies confirmed that amurensin G treatment suppresses MDR1 expression in tumor tissues and rescues doxorubicin responsiveness.

In our preliminary study, we found that the promoter region of the MRP2 gene contained four FoxO binding sites and FoxO1 overexpression enhanced gene transcription. Moreover, amurensin G suppressed both MRP2 protein expression and gene transcription in MRP2-overexpressing, tamoxifen-resistant breast cancer cells (Supplemental Fig. 1). Although more studies to establish of the regulatory mechanism for amurensin G effects may be useful (for example by investigating other potential molecular targets such as the PI3-kinase/Akt pathway), nevertheless our study establishes that SIRT1 inhibitors influence FoxO1 activation and subsequently affect MDR transporters.

Overall, our data show that SIRT1 plays an important role in MDR1 gene transcription via FoxO1 activity and suggest that SIRT1 could be a new therapeutic target to overcome chemoresistance. A potent SIRT1 inhibitor, amurensin G identified from screening a phytochemical library appears to have therapeutic potential as a new type of inhibitor of multidrug resistance.

References

Accili D and Arden KC (2004) FoxOs at the crossroads of cellular metabolism, differentiation, and transformation. *Cell* **117**:421-426.

Ahn MY, Chung HY, Choi WS, Lee BM, Yoon S and Kim HS (2010) Anti-tumor effect of apicidin on Ishikawa human endometrial cancer cells both in vitro and in vivo by blocking histone deacetylase 3 and 4. *Int J Oncol* **36**:125-131.

Alcaín FJ and Villalba JM (2009) Sirtuin inhibitors. *Expert Opin Ther Pat* **19**:283-294.

Arden KC (2006) Multiple roles of FOXO transcription factors in mammalian cells point to multiple roles in cancer. *Exp Gerontol* **41**:709-717.

Asada S, Daitoku H, Matsuzaki H, Saito T, Sudo T, Mukai H, Iwashita S, Kako K, Kishi T, Kasuya Y and Fukamizu A (2007) Mitogen-activated protein kinases, Erk and p38, phosphorylate and regulate Foxo1. *Cell Signal* **19**:519-527.

Barthel A, Schmoll D and Unterman TG (2005) FoxO proteins in insulin action and metabolism. *Trends Endocrinol Metab* **16**:183-189.

Bodó A, Bakos E, Szeri F, Váradi A and Sarkadi B (2003) The role of multidrug transporters in drug availability, metabolism and toxicity. *Toxicol Lett* **140-141**:133-143.

Borra MT, Smith BC and Denu JM (2005) Mechanism of human SIRT1 activation by resveratrol. *J Biol Chem* **280**:17187-17195.

Brown DC, Gatter KC, Mason DY (1990) Proliferation in non-Hodgkin's lymphoma: a comparison of Ki-67 staining on fine needle aspiration and cryostat sections. *J Clin Pathol* **43:**325-328.

Daitoku H, Hatta M, Matsuzaki H, Aratani S, Ohshima T, Miyagishi M, Nakajima T and Fukamizu A (2004) Silent information regulator 2 potentiates Foxo1-mediated

transcription through its deacetylase activity. *Proc Natl Acad Sci USA* **101**:10042-10047.

de Boer VC, de Goffau MC, Arts IC, Hollman PC and Keijer J (2006) SIRT1 stimulation by polyphenols is affected by their stability and metabolism. *Mech Ageing Dev* **127**:618-627.

Frescas D, Valenti L and Accili D (2005) Nuclear trapping of the forkhead transcription factor FoxO1 via Sirt-dependent deacetylation promotes expression of glucogenetic genes. *J Biol Chem* **280**:20589-20595.

Gan L, Han Y, Bastianetto S, Dumont Y, Unterman TG and Quirion R (2005) FoxO-dependent and -independent mechanisms mediate SirT1 effects on *IGFBP-1* gene expression. *Biochem Biophys Res Commun* **337**:1092-1096.

Glavinas H, Krajcsi P, Cserepes J and Sarkadi B (2004) The role of ABC transporters in drug resistance, metabolism and toxicity. *Curr Drug Deliv* **1**:27-42.

Gottesman MM, Fojo T, Bates SE (2002) Multidrug resistance in cancer: role of ATP-dependent transporters. *Nat Rev Cancer* **2:**48-58.

Grozinger CM, Chao ED, Blackwell HE, Moazed D and Schreiber SL (2001) Identification of a class of small molecule inhibitors of the Sirtuin family of NAD-dependent deacetylases by phenotypic screening. *J Biol Chem* **276**:38837-38843.

Ha D, Chen Q, Hung T, Youn U, Ngoc T, Thuong P, Kim H, Seong Y, Min B and Bae K (2009) Stilbenes and oligostilbenes from leaf and stem of *Vitis amurensis* and their cytotoxic activity. *Arch Pharm Res* **32**:177-183.

Han CY, Cho KB, Choi HS, Han HK and Kang KW (2008) Role of FoxO1 activation in MDR1 expression in adriamycin-resistant breast cancer cells. *Carcinogenesis* **29**:1837-1844.

Hoekman MF, Jacobs FM, Smidt MP and Burbach JP (2006) Spatial and temporal expression of FoxO transcription factors in the developing and adult murine brain. *Gene Expr Patterns* **6**:134-140.

Kobayashi Y, Furukawa-Hibi Y, Chen C, Horio Y, Isobe K, Ikeda K and Motoyama N (2005) SIRT1 is critical regulator of FOXO-mediated transcription in response to oxidative stress. *Int J Mol Med* **16**:237-243.

Kuo MT (2007) Roles of multidrug resistance genes in breast cancer chemoresistance. *Adv Exp Med Biol* **608**:23-30.

Lage H (2003) ABC-transporters: implications on drug resistance from microorganisms to human cancers. *Int J Antimicrob Agents* **22**:188-199.

Lara E, Mai A, Calvanese V, Altucci L, Lopez-Nieva P, Martinez-Chantar ML, Varela-Rey M, Rotili D, Nebbioso A, Ropero S, Montoya G, Oyarzabal J, Velasco S, Serrano M, Witt M, Villar-Garea A, Imhof A, Mato JM, Esteller M and Fraga MF (2009) Salermide, a Sirtuin inhibitor with a strong cancer-specific proapoptotic effect. *Oncogene* **28**:781-791.

Ling V (1997) Multidrug resistance: molecular mechanisms and clinical relevance. *Cancer Chemother Pharmacol* **40 Suppl**:S3-S8.

Liu F, Xie ZH, Cai GP and Jiang YY (2007) The effect of survivin on multidrug resistance mediated by P-glycoprotein in MCF-7 and its adriamycin resistant cells. *Biol Pharm Bull* **30**:2279-2283.

Motta MC, Divecha N, Lemieux M, Kamel C, Chen D, Gu W, Bultsma Y, McBurney

M and Guarente L (2004) Mammalian SIRT1 represses forkhead transcription factors. *Cell* **116**:551-563.

Ota H, Tokunaga E, Chang K, Hikasa M, Iijima K, Eto M, Kozaki K, Akishita M, Ouchi Y and Kaneki M (2006) Sirt1 inhibitor, Sirtinol, induces senescence-like growth arrest with attenuated Ras-MAPK signaling in human cancer cells. *Oncogene* **25**:176-185.

Ozben T (2007) Oxidative stress and apoptosis: impact on cancer therapy. *J Pharm Sci* **96**:2181-2196.

Pérez-Tomás R (2006) Multidrug resistance : retrospect and prospects in anti-cancer drug treatment. *Curr Med Chem* **13**:1859-1876.

Reagan-Shaw S and Ahmad N (2007) The role of Forkhead-box Class O (FoxO) transcription factors in cancer: a target for the management of cancer. *Toxicol Appl Pharmacol* **224**:360-368.

Saunders LR and Verdin E (2007) Sirtuins: critical regulators at the crossroads between cancer and aging. *Oncogene* **26**:5489-5504.

Schreiber E, Harshman K, Kemler I, Malipiero U, Schaffner W and Fontana A (1990) Astrocytes and glioblastoma cells express novel octamer-DNA binding proteins distinct from the ubiquitous Oct-1 and B cell type Oct-2 proteins. *Nucleic Acids Res* **18**:5495-5503.

Sharom FJ (2008) ABC multidrug transporters: structure, function and role in chemoresistance. *Pharmacogenomics* **9**:105-127.

Stünkel W, Peh BK, Tan YC, Nayagam VM, Wang X, Salto-Tellez M, Ni B, Entzeroth M and Wood J (2007) Function of the SIRT1 protein deacetylase in cancer. *Biotechnol J* **2**:1360-1368.

Vellonen KS, Honkakoski P and Urtti A (2004) Substrates and inhibitors of efflux proteins interfere with the MTT assay in cells and may lead to underestimation of drug toxicity. *Eur J Pharm Sci* **23**:181-188.

Vogt PK, Jiang H and Aoki M (2005) Triple layer control: phosphorylation, acetylation and ubiquitination of FOXO proteins. *Cell Cycle* **4**:908-913.

Yeung F, Hoberg JE, Ramsey CS, Keller MD, Jones DR, Frye RA and Mayo MW (2004) Modulation of NF-kappaB-dependent transcription and cell survival by the SIRT1 deacetylase. *EMBO J* **23**:2369-2380.

Zhou J, Liu M, Aneja R, Chandra R, Lage H and Joshi HC (2006) Reversal of P-glycoprotein-mediated multidrug resistance in cancer cells by the c-Jun NH2-terminal kinase. *Cancer Res* **66**:445-452.

FOOTNOTES

First two authors (Oh WK and Cho KB) equally contributed to this work.

This work was supported by National Research Foundation of Korea grants funded by the Korea government (2009-0083757, 2010-0001707 and R13-2008-010-01001-0).

Molecular Pharmacology Fast Forward. Published on August 16, 2010 as DOI: 10.1124/mol.110.065961
This article has not been copyedited and formatted. The final version may differ from this version.

Figure Legends

Fig. 1. Role of SIRT1 in MDR1 gene transcription. (A) Transactivation of *MDR1* gene by SIRT1 overexpression. Reporter activity of p195-MDR1 (left panel) and MDR1 protein expression (right panel) in MCF-7 cells transiently transfected with SIRT1-CA (30-300 ng/well) or pCMV5 (mock transfection, 300 ng) plasmid. Data represents means ± SD with 4 different samples (significant versus the control, *p<0.05; **p<0.01). (B) FoxO1 activation by SIRT1 overexpression. Reporter activity of FHRE reporter (left panel) in MCF-7 cells transiently transfected with FHRE minimal reporter plasmid in combination with SIRT1-CA (30-300 ng/well) or pCMV5 (mock transfection, 300 ng) plasmid. Data represents means ± SD with 4 different samples (significant versus the control, *p<0.05; **p<0.01). Nuclear levels of FoxO1 and FoxO3a (right panel) in MCF-7 cells transiently transfected with SIRT1-CA (30-300 ng/well) or pCMV5 (mock transfection, 300 ng) plasmid. Western blot analysis was performed using nuclear extracts obtained from both the cells serum-starved for 24 h after transfection, and the levels of FoxO1 and Fox3a in the nuclear fractions were immunochemically detected using specific antibodies. (C) Effect of SIRT1 inhibitor on FoxO1-mediated MDR1 expression. Immunoblot analyses (left panel). Representative immunoblots show protein expression of MDR1 and nuclear FoxO1 and FoxO3 in both MCF-7 and MCF-7/ADR cells incubated with or without 1 mM nicotinamide (NAM) for 24 h. Equal loading of proteins was verified by actin or lamin B1 immunoblot. Rhodamine-123 retention assay (right panel). After incubation of MCF-7 and MCF-7/ADR cells with 20 μM R-123 for 90 min, the R-123 fluorescence values in cell lysates were measured using the excitation and emission wavelengths of 480 and 540 nm, respectively. 1 mM NAM was

Molecular Pharmacology Fast Forward. Published on August 16, 2010 as DOI: 10.1124/mol.110.065961
This article has not been copyedited and formatted. The final version may differ from this version.

added 24 h before rhodamine-123 loading. The values were divided by total protein contents of each sample. Data represents means ± SD of 4 separate samples (significant versus the control MCF-7 cells, **p<0.01; significant versus the vehicle-treated MCF-7/ADR cells, $^{\#}$p<0.05).

Fig. 2. The complementary effects of FoxO1 and SIRT1. (A) Up-regulation of MDR1 transactivation by FoxO1 with or without SIRT1 overexpression. MCF-7 cells were co-transfected with p195-MDR1 reporter and pCMV5-FoxO1 (30 ng/well) in the presence or absence of SIRT1 overexpression plasmid (SIRT1-CA, 300 ng/well) and then the luciferase activities were measured 18 h after transfection (left panel). Data represent the means ± SD of 3 different samples (significant versus the pCMV5-transfected MCF-7 cells, **p<0.01; significant versus the FoxO1-trasnfected MCF-7 cells, $^{\#\#}$p<0.01). Immunoblot analysis of MDR1 (right penel). MCF-7 cells were transfected with pCMV5-FoxO1 (100 ng/well) in the presence or absence of SIRT1 overexpression plasmid (300 ng/well) and then the total cell lysates were obtained 24 h after transfection. (B) Reversion of SIRT1 induced *MDR1* gene transcription by FoxO1 suppression. p195-MDR1 reporter activities were measured in MCF-7 cells co-transfected with 300 ng/well pCMV5 or SIRT1-CA in combination with control siRNA or FoxO1 siRNA (20 *p*mole/well, left panel). Data represents means ± SD with 3 different samples (significant versus the control siRNA and pCMV5-transfected MCF-7 cells, **p<0.01; significant versus the control siRNA and SIRT1-transfected MCF-7 cells, $^{\#\#}$p<0.01). Immunoblot analysis of MDR1 (right penel). MCF-7 cells were co-transfected with 300 ng/well SIRT1-CA with 60 *p*g/well control siRNA or FoxO1 siRNA and then the total cell lysates were obtained 24 h after transfection.

Molecular Pharmacology Fast Forward. Published on August 16, 2010 as DOI: 10.1124/mol.110.065961
This article has not been copyedited and formatted. The final version may differ from this version.

Fig. 3. MDR1 inhibition by amurensin G, a natural SIRT1 inhibitor. (A) Structures of amurensin G. (B) *In vitro* SIRT1 inhibition by amurensin G and nicotinamide (left panel). FHRE reporter activity (right panel). MCF-7 cells were co-transfected with FHRE reporter plasmid with pCMV5 or SIRT1 (300 ng). 6 h after transfection, the cells were incubated with vehicle dimethylsulfoxide or amurensin G (0.1-1 μg/ml) for further 18 h. Data represent the means ± SD of 3 different samples (significant versus the pCMV5-transfected MCF-7 cells, $^{**}p<0.01$; significant versus the SIRT1-trasnfected and vehicle-treated MCF-7 cells, $^{\#}p<0.05$; $^{\#\#}p<0.01$). (C) Inhibitory effect of amurensin G on FoxO1-induced MDR1 expression. MCF-7/ADR cells were incubated with or without amurensin G (0.3-3 μg/ml) for 24 h and total cell lysates and nuclear fractions were subjected to immunoblottings for MDR1, FoxO1 and FoxO3. (D) Cell viability change after treating MCF-7/ADR cells with amurensin G. After incubation of MCF-7/ADR cells with or without amurensin G (0.1-3 μg/ml) for 24 h, cell viabilities were determined by using MTT assay. Data represent the means ± SD of 14 different samples.

Fig. 4. Overcome of doxorubicin resistance in MCF-7/ADR cells by amurensin G. (A) Cellular doxorubicin uptake. After incubation of MCF-7 and MCF-7/ADR cells with or without amurensin G (0.1-3 μg/ml) for 24 h, doxorubicin (30 μM) was treated for 60 min. Doxorubicin fluorescence intensities retained in cell lysates of MCF-7 and MCF-7/ADR were measured using the excitation and emission wavelengths of 470 and 590 nm, respectively. The values were divided by total protein content of each sample. Data represent the means ± SD of 3 different samples (significant versus the untreated MCF-7/ADR cells, $^{*}p<0.05$; $^{**}p<0.01$; control level = 1). (B) Intracellular concentration

of doxorubicin. After incubation of MCF-7 and MCF-7/ADR cells with or without amurensin G (0.1-3 μg/ml) for 24 h, doxorubicin (30 μM) was treated for 60 min and intracellular concentration of doxorubicin was measured as described in method section. The values were divided by total protein content of each sample. Data represent the means ± SD of 4 different samples (significant versus the untreated MCF-7/ADR cells, *p<0.05; **p<0.01). (C) Synergistic cytotoxicity by amurensin G and doxorubicin in MCF-7/ADR cells. Amurensin G (0.1-1 μg/ml) was preincubated for 24 h and MCF-7 and MCF-7/ADR cells were exposed to doxorubicin (30 μM) for additional 24 h. Cell viabilities were determined by crystal violet assay. Data represent the means ± SD of 14 different samples (significant versus the doxorubicin alone-treated MCF-7/ADR cells, **p<0.01). (D) Potentiation of doxorubicin-mediated DNA synthesis inhibition by amurensin G. MCF-7/ADR cells were treated same as described in panel C and BrdU assays were performed. Data represent the mean ± SD of 8 different samples (significant versus the doxorubicin alone-treated MCF-7/ADR cells, **p<0.01). (E) Representative photographs of TUNEL assays on cells cultured with or without 30 μM doxorubicin for 24 h. MCF-7/ADR cells were pretreated with CPP343 (0.3-1 μg/ml) 24 h before doxorubicin exposure. (F) Synergistic cell proliferation inhibition by amurensin G and paclitaxel (Taxol) in MCF-7/ADR cells. Amurensin G (0.1-1 μg/ml) was preincubated for 24 h and MCF-7/ADR cells were exposed to doxorubicin (30 μM) for additional 48 h in 10% FBS-containing medium. Relative cell number was determined by MTT assay. Data represent the means ± SD of 8 different samples (significant versus the paclitaxel alone-treated MCF-7/ADR cells, **p<0.01).

Fig. 5. Restoration of doxorubicin responsiveness by amurensin G in xenograft study.

(A) MCF-7/ADR tumor growth inhibition by amurensin G. Representative photographs of tumor bearing athymic mice treated with or without doxorubicin (4 mg/kg, i.p., once a week for four weeks) and amurensin G (10 mg/kg, i.p. two times a week for four weeks)(upper panel). Tumor size was determined by caliper measurements every 3 days and their volumes calculated using a standard formula: $width^2$ x length x 0.52. Data were expressed as the means ± SD of 4 different mice (significant versus the untreated control, *p<0.05, **p<0.01; significant versus the doxorubicin alone-treated group, $^{\#}$p<0.05, $^{\#\#}$p<0.01). (B) Histology and immunohistochemistry of tumor tissues. H&E staining, immunohistochemical staining for PCNA, Ki-67 and TUNEL staining on paraffin sections from solid tumor tissues. The value in each picture represents means ± SD of 4 different samples (significant versus the doxorubicin alone-treated group, *p<0.05, **p<0.01). (C) MDR1 expression in tumor tissue lysates. Tumor tissues were homogenized in PBS and centrifuged at 10,000g. The supernatants were subjected to immunoblottings. Each lane was loaded with 20 μg of the tissue lysates. Equal protein loading was verified using actin as an internal standard. The results were confirmed by 2 separate experiments.

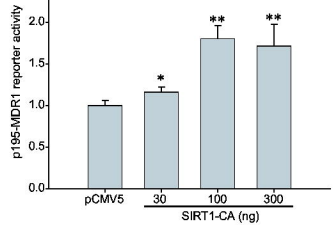
p195-MDR1 reporter activity
2.0
1.5
1.0
0.5
0.0
*
**
**
pCMV5
30
100
300
SIRT1-CA (ng)

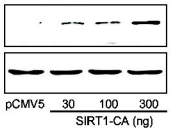
MDR1
Actin
pCMV5
30
100
300
SIRT1-CA (ng)

B

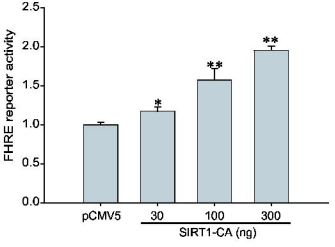
FHRE reporter activity
2.5
2.0
1.5
1.0
0.5
0.0
*
**
**
pCMV5
30
100
300
SIRT1-CA (ng)

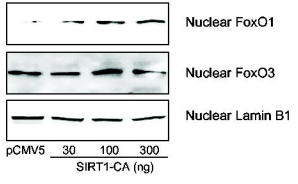
Nuclear FoxO1
Nuclear FoxO3
Nuclear Lamin B1
pCMV5
30
100
300
SIRT1-CA (ng)

C

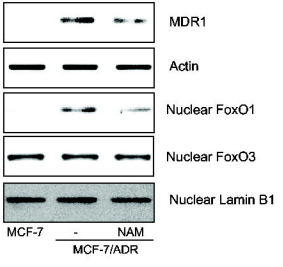
MDR1
Actin
Nuclear FoxO1
Nuclear FoxO3
Nuclear Lamin B1
MCF-7
-
NAM
MCF-7/ADR

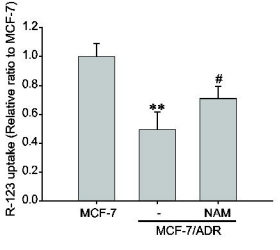
R-123 uptake (Relative ratio to MCF-7)
1.2
1.0
0.8
0.6
0.4
0.2
0.0
**
#
MCF-7
-
NAM
MCF-7/ADR

Fig. 1

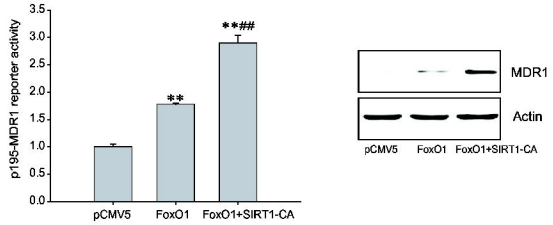
p195-MDR1 reporter activity
3.5
3.0
2.5
2.0
1.5
1.0
0.5
0.0
**
**##
pCMV5
FoxO1
FoxO1+SIRT1-CA
MDR1
Actin
pCMV5
FoxO1
FoxO1+SIRT1-CA

B

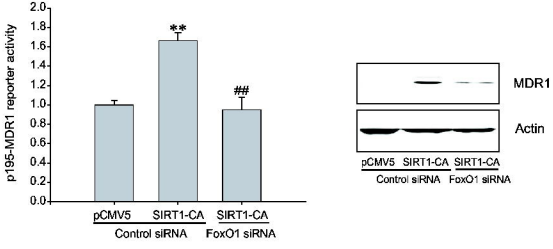
p195-MDR1 reporter activity
2.0
1.8
1.6
1.4
1.2
1.0
0.8
0.6
0.4
0.2
0.0
**
##
pCMV5
SIRT1-CA
SIRT1-CA
Control siRNA
FoxO1 siRNA
MDR1
Actin
pCMV5
SIRT1-CA
SIRT1-CA
Control siRNA
FoxO1 siRNA

Fig. 2

Molecular Pharmacology Fast Forward. Published on August 16, 2010 as DOI: 10.1124/mol.110.065961
This article has not been copyedited and formatted. The final version may differ from this version.

A

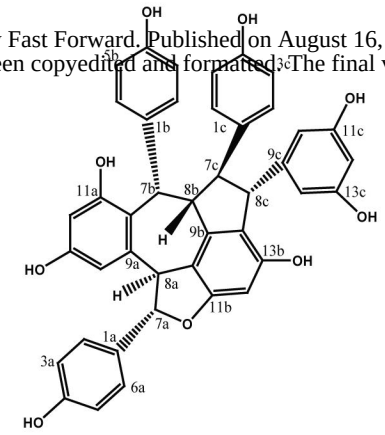

Amurensin G

B

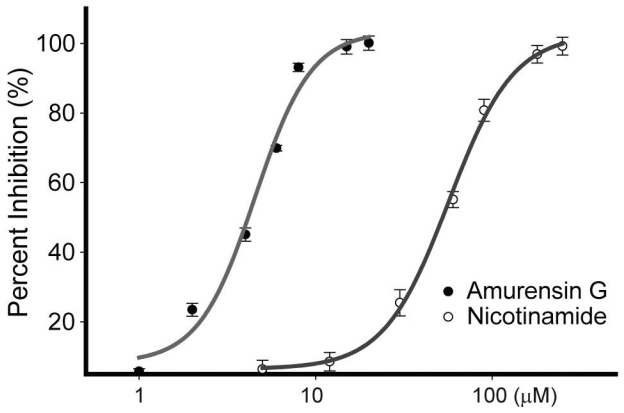

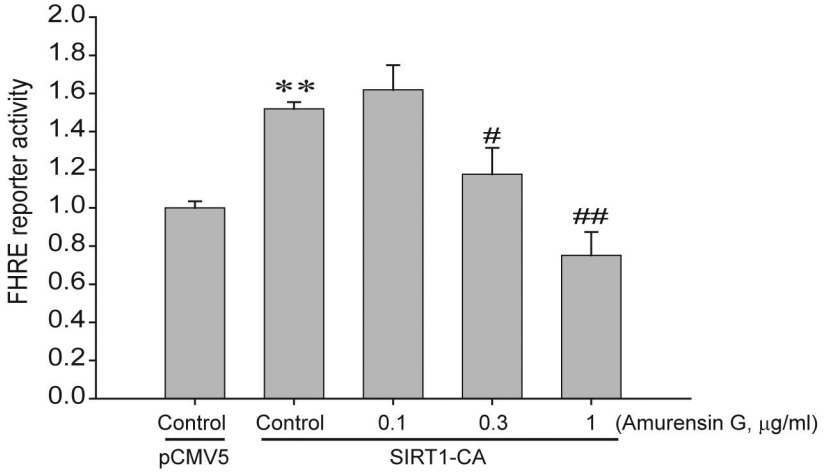

C

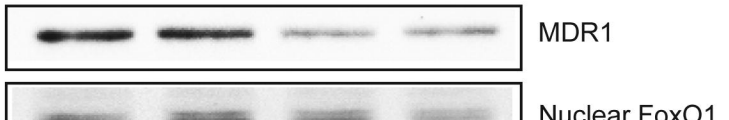

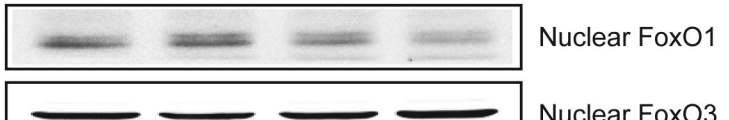

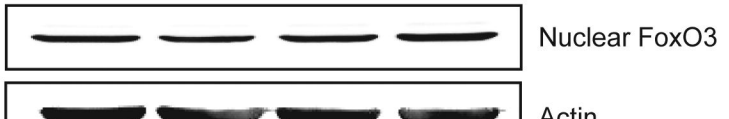

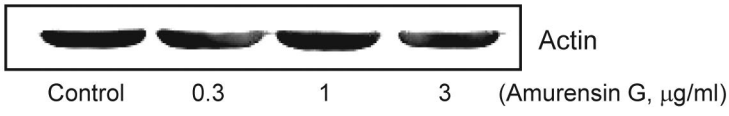

D

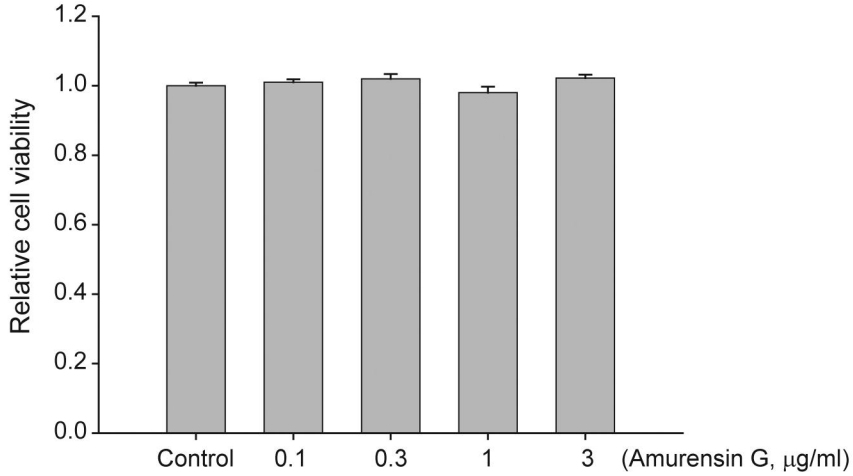

Fig. 3

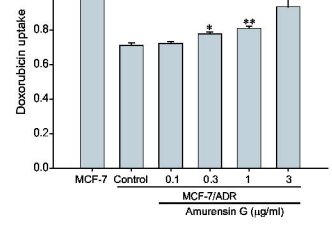
Doxorubicin uptake
MCF-7
Control
0.1
0.3
1
3
MCF-7/ADR
Amurensin G (μg/ml)

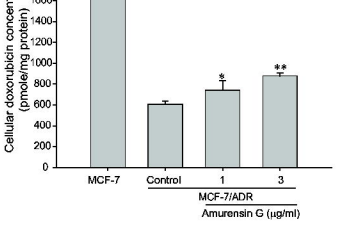
Cellular doxorubicin concentration (pmole/mg protein)
MCF-7
Control
1
3
MCF-7/ADR
Amurensin G (μg/ml)

C

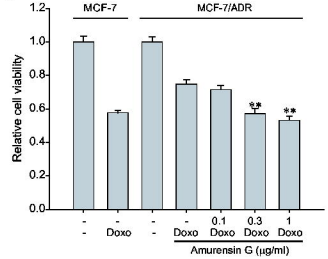
MCF-7
MCF-7/ADR
Relative cell viability
Doxo
0.1
0.3
1
Amurensin G (μg/ml)

D

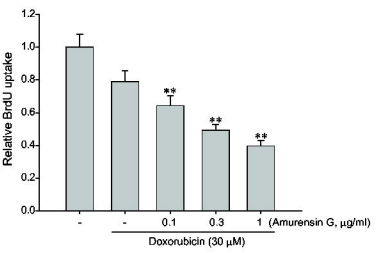
Relative BrdU uptake
0.1
0.3
1 (Amurensin G, μg/ml)
Doxorubicin (30 μM)

E

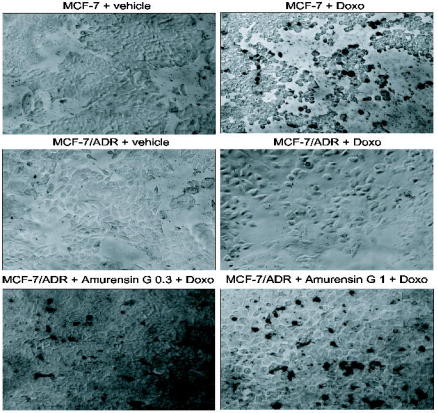
MCF-7 + vehicle
MCF-7 + Doxo
MCF-7/ADR + vehicle
MCF-7/ADR + Doxo
MCF-7/ADR + Amurensin G 0.3 + Doxo
MCF-7/ADR + Amurensin G 1 + Doxo

F

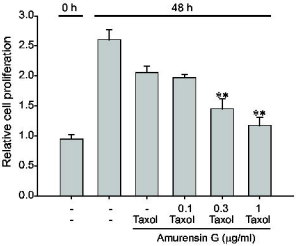
0 h
48 h
Relative cell proliferation
Taxol
0.1
0.3
1
Amurensin G (μg/ml)

Fig. 4

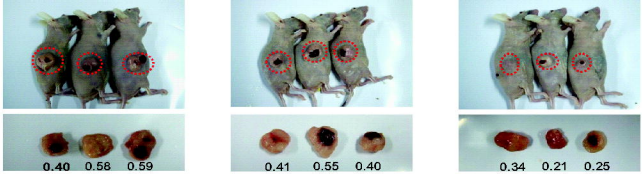
Tumor weight (g)
0.40 0.58 0.59
0.41 0.55 0.40
0.34 0.21 0.25

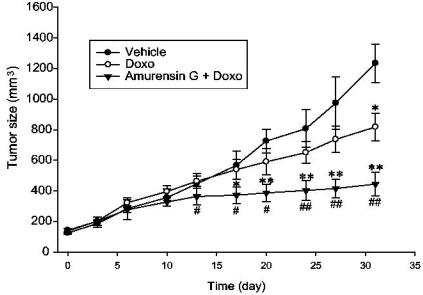
Vehicle
Doxo
Amurensin G + Doxo
Tumor size (mm3)
Time (day)

B

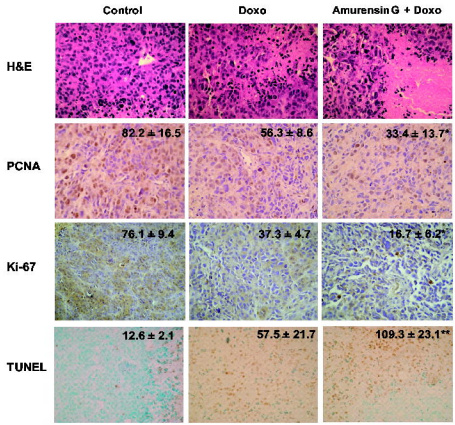
Control
Doxo
Amurensin G + Doxo
H&E
PCNA
82.2 ± 16.5
56.3 ± 8.6
33.4 ± 13.7*
Ki-67
76.1 ± 9.4
37.3 ± 4.7
16.7 ± 6.2*
TUNEL
12.6 ± 2.1
57.5 ± 21.7
109.3 ± 23.1**

C

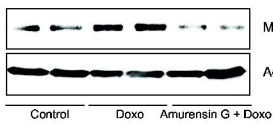
MDR1
Actin
Control
Doxo
Amurensin G + Doxo

Fig. 5